ON THE GEOMETRIC ACCURACY OF SOME DIFFERENTIAL-TYPE OF EDGE DETECTORS AND NON-LINEAR SMOOTHING FILTERS

Mathias J.P.M. Lemmens & C. San L.A. Han

Delft University of Technology, Faculty of Geodesy,
Institute of Photogrammetry and Remote Sensing,
Thijsseweg 11, 2629 JA Delft, The Netherlands

Comm. III/4

Abstract: The accuracy of edge detectors in combination with non-linear smoothing filters is considered and their precision experimentally investigated. A synthetic 128 x 128 pixel image, consisting of triangle-shaped objects and ideal step edges, is used as true image. The image is artificially distorted by blur, Gaussian noise and impulse noise. The influence of these distortions on edge location position is investigated for several edge detectors (the Prewitt, the Sobel and the Normal gradient operator) in combination with the median, edge preserving and conditional average filter. The Prewitt and Sobel operator show nearly the same characteristics. The Normal gradient performs well under nearly noise free conditions and also under heavy noise when combined with the edge preserving or conditional average filter. The median filter is superior to the other filters under heavy noise conditions, with respect to precision, but many edges are undetected. The edge preserving filter has the most consistent behaviour.

1 Introduction

Images are the most important data source to achieve spatial information. Information extraction from images involves four steps: (1) image formation, (2) preprocessing, (3) analysis and (4) presentation and storage. Lemmens (1988) gives a comprehensive description.

There are many phenomena that may degrade the image during image formation. Degradation compels preprocessing. If the degradation sources are known and can be adequately described, a restoration procedure can be started. But very often no or insufficient knowledge about the degradation process is available; just enhancement techniques remain. Important enhancement methodes in the present investigation are smoothing filters.

Analysis is a two stage process: (1) segmentation and (2) pattern recognition. Although there exist other segmentation techniques, e.g. histogram thresholding and region growing, the most fundamental one for a majority of image processing tasks is boundary detection, i.e. tracing of boundaries between regions which are homogeneous in grey value and/or texture. Boundary detection consists of two steps: (1) edge detection and (2) line following.

The aim of this paper is to investigate systematically the precision of edge location of, in particular, three differential-type of edge operators in combination with some non-linear smoothing filter as function of several types of degradation. In fig. 1 the scheme of the investigation is shown.

The edge detectors under present consideration are: (1) Prewitt operator, (2) Sobel operator and (3) Normal gradient operator. Also three types of non-linear smoothing filters are looked at: (1) median filter, (2) edge preserving filter and (3) conditional average filter.

Experiments are carried out on synthetic images, size 128 x 128 pixels, containing 23 triangles of different sizes, shapes and orientations, against a uniform background. This ideal image is artificially degraded by: (1) Gaussian noise (sigma = 5, 10 and 20), (2) impulse noise (1 % and 5 %) and (3) blur (simulated by a 3 x 3 Gaussian weighted linear smoothing filter.). The edges are constructed as ideal step edges. Just edges between region wich differ in grey value are considered. No texture boundaries are investigated. As precision measure of edge location the average distance between the detected edges and the lines in the ideal image is employed.

First, in the next section, some preliminaries on edge detection and smoothing filters are given. Next, the performance of the ideal image, the simulation of the degradations and the applied precision measure are treated. Section 4 gives the experimental results and discusses them.

2 Edge Detectors and Smoothing Filters

2.1 Edge Detectors

Edge detection is part of boundary detection; a segmentation process. Extraction of boundaries comprises:

- detection of local edges (edge detection);
- aggregration of the edgels (= edge elements) to lines on the basis of grouping criteria (line following).

Edges are usually defined as local discontinuities or abrupt changes in image grey values and/or texture. We only consider here abrupt grey value changes.

Edge detection is a filter operator on images, which attributes to each pixel a probability that the edgel is part of a real boundary. Commonly the edge strength or magnitude is used to indicate the edge probability. Often just a threshold on the edge magnitude is employed; all pixels with magnitudes above the threshold are part of a boundary, the other ones are not. It is possible to apply a less rigorous method by incorporating the edge strength of the neighbour pixels to decrease or augment the probability. This completion leads to edge relaxation (cf. Lemmens et al., 1988). In the present investigation a threshold is used. This can be done without objection, since the characteristics of the ideal image are well known.

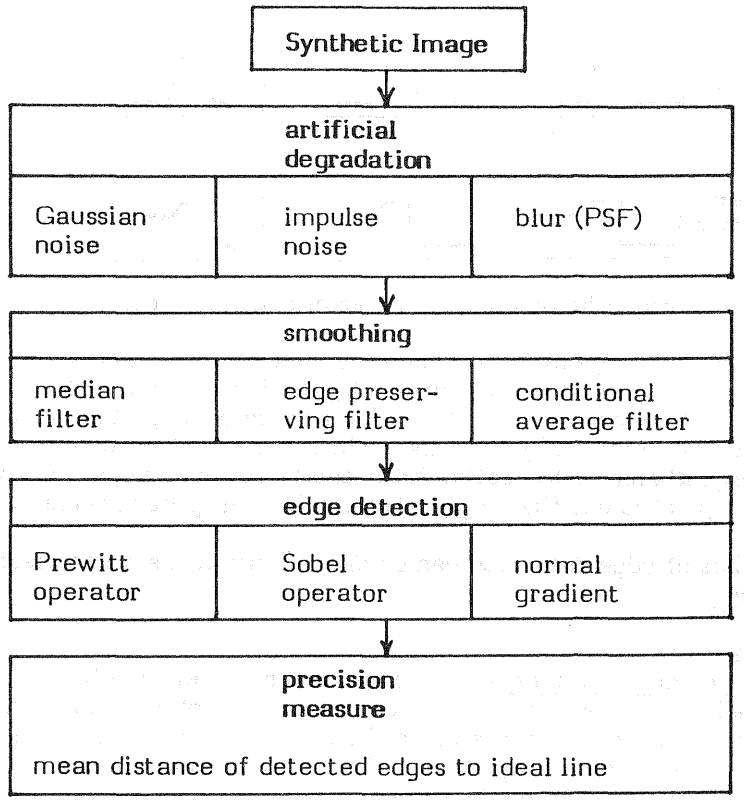

Fig. 1 Schematic review

Smith and Davis (1975) have summarized some characteristics of edge detection:

1 isotropy (i.e. the insensitivety to edge orientation);
2 edge type response (i.e. behaviour under different type of edges);
3 dynamic range of the grey values (i.e. the effectiveness over varying grey value changes);
4 responses under noise conditions;
5 adaptability to different image conditions during processing;
6 computational aspects (time and storage aspects, machine independency).

Our aim is to investigate the effect of characteristics 1-4 on edge location. We have extended point 4 (noise condition) to a more general notion: degradation conditions. Davis (1975) distinguishes three types of edge degradation factors:

1 photon noise;
2 blurring;
3 texture.

In the present investigation noise and blurring are considered, with an emphasis on noise. Since edges are detected by operators which are usually of small size with respect to the image, edge detection is extremely sensitive to noise. Noise can be caused by very different phenomena, e.g. bit reversal during transfer of the digital signal, photographic graininess, quantization noise and defective sensor elements. There are many types of edges, e.g. ramp edge, ideal step edge, roof edge and spike edge. Fig. 2 shows some common types of edge profiles. Here, ideal step edges are considered. Although investigations on the influence of edge orientation on edge location and the difference between object and background grey values are foreseen, they are yet not a part of the present investigation.

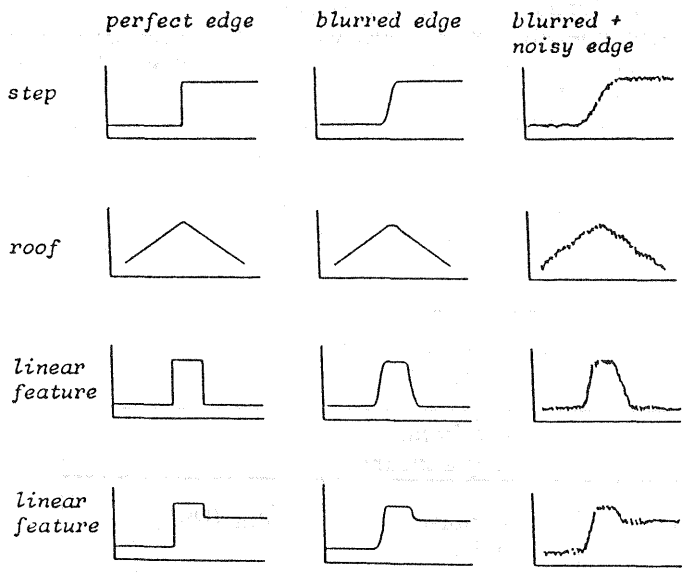

Fig. 2 Some common types of edge profiles.

Since the performance of edge detection requires both an image model and an edge model, it is a severe problem to deal with. This is affirmed by the large number of approaches published in the open literature, with which one has attempted to tackle the problem. None of the approaches has proven to be fully satisfying and this again leads to the frequent publication of "new approaches" (e.g. Morgenthaler, 1981; Sethi, 1982; and Smith and Davis, 1975). Recently, Torre and Poggio (1986) have pointed out that edge detection is an ill-posed problem.

The common approaches of edge detection can be divided into three broad classes:
- template matching;
- differentation;
- variance analysis.

The background of template matching is to compute the correlation between an image patch and masks corresponding to ideal step edges in a selected number of directions. Denoting the image patch signal by X and the template signal Y, the most simple correlation function is employed: discrete correlation, defined by: Σ X.Y. The mask giving the highest output is the response and defines also the direction of the edge.

The variance analysis is also often called moment analysis. The variances of the grey values are determined in several directions or the eigenvalues of the covariance matrix of some local difference function of grey values is evaluated. The operator described by Förstner (1986) is an example of the last kind.

The differential method computes the gradient of the grey values of a local neighbourhood. There are two approaches:
- derivation of discrete differentation from the continuous case (gradient method);
- approximation of the local grey value function by a least squares surface fitting and computation of the gradient of the fit (surface fitting).

The gradients are computed in two perpendicular directions, commonly corresponding with the rows and columns of the image matrix, leading to g_x and g_y. However, the Roberts gradient employes the diagonals as principal directions. The commonly employed edge responses, use the fact that g_x and g_y define a 2-D vector field, for which a distance and an orientation can be defined.

The distance measure leads to the edge strength or magnitude:

$$M = (g_x^2 + g_y^2)^{\frac{1}{2}}$$

The gradient orientation is defined by:

$$D = \text{atan} (g_y / g_x)$$

To save computation time often less time-consuming approximations of edge strength are used:

$$M' = | g_x | + | g_y |$$

or:

$$M'' = \max (| g_x | , | g_y |)$$

The above measures may be considered as special cases of the Minkowski general expression for distances in a metric n-dimensional space. Let L(a,b) denote the distance between a and b, with coordinates: X_i^a and X_i^b, i = 1,..,n, respectively. Then:

$$L(a,b) = (\sum_{i=1}^{n} | X_i^a - X_i^b |^p)^{1/p} = (\sum_{i=1}^{n} |\Delta X_i|^p)^{1/p}$$

For n = 2, L(a,b) becomes for:

$$p = 1: \quad L(a,b) = | \Delta X_1 | + | \Delta X_2 |$$

$$p = 2: \quad L(a,b) = (\Delta X_1^2 + \Delta X_2^2)^{\frac{1}{2}}$$

$$p = \infty: \quad L(a,b) = \max (|\Delta X_1| , |\Delta X_2|)$$

A third kind of edge response, which will depend on the size of the operator and the kind of edge, is the edge width. The larger the operator size, the larger the edge width. A ramp edge or a blurred ideal step edge will show broad edge responses and small edge strength magnitudes.

For the gradient method, according to the differentation of a continuous signal, differentation of a discrete signal is defined. One of the most common schemes is:

$$\frac{d\, g(i,j)}{d\, x} = g_x = g(i,j) - g(i-1,j)$$

$$\frac{d\, g(i,j)}{d\, y} = g_y = g(i,j) - g(i,j-1)$$

leading to the convolution masks: $-1 \quad \underline{1}$ and $\begin{matrix} -1 \\ \underline{1} \end{matrix}$ (see fig. 3), i.e.:

$$g_x = g * \begin{matrix} -1 & \underline{1} \end{matrix} \quad ; \quad g_y = g * \begin{matrix} -1 \\ \underline{1} \end{matrix}$$

The second approach of the differential-type of edge detection is by least squares surface fitting of the local grey value function. The surface is e.g. a (tilted) plane or a quadratic or even a higher order polynomial surface. The method actually requires an edge model. Common models are ramp edges. The least squares adjustment enables a hyptohesis testing on the assumed edge model (Haralick, 1980).

The original Roberts gradient is derived from the approximation of a 2 x 2 neighbourhood by a plane, leading to two perpendicular gradient masks:

$$g_x: \begin{matrix} -1 & 1 \\ -1 & 1 \end{matrix} \quad \text{and} \quad g_y: \begin{matrix} -1 & -1 \\ 1 & 1 \end{matrix}$$

The Roberts' gradient is usually applied as a linear combination of g_x and g_y:

$$g_u = \tfrac{1}{2} (g_x + g_y) \quad \text{and} \quad g_v = -\tfrac{1}{2} (g_x - g_y)$$

leading to the masks: $g_u: \begin{matrix} -1 & 0 \\ 0 & 1 \end{matrix}$ and $g_v: \begin{matrix} 0 & -1 \\ 1 & 0 \end{matrix}$

The Prewitt operator is originally derived from a second order polynomial surface fit within a 3 x 3 neighbourhood. The masks are shown in fig. 3. For a 3 x 3 window these masks are the same as for a surface approximation of the local image function by a tilted plane. Hueckel (1973) employs the surface fitting approach by using low-frequency polar-form Fourier basic functions on a circular disk in order to detect step edges. In the present investigation, the Prewitt operator, the Sobel operator and the normal gradient are regarded. Their masks are shown in fig. 3

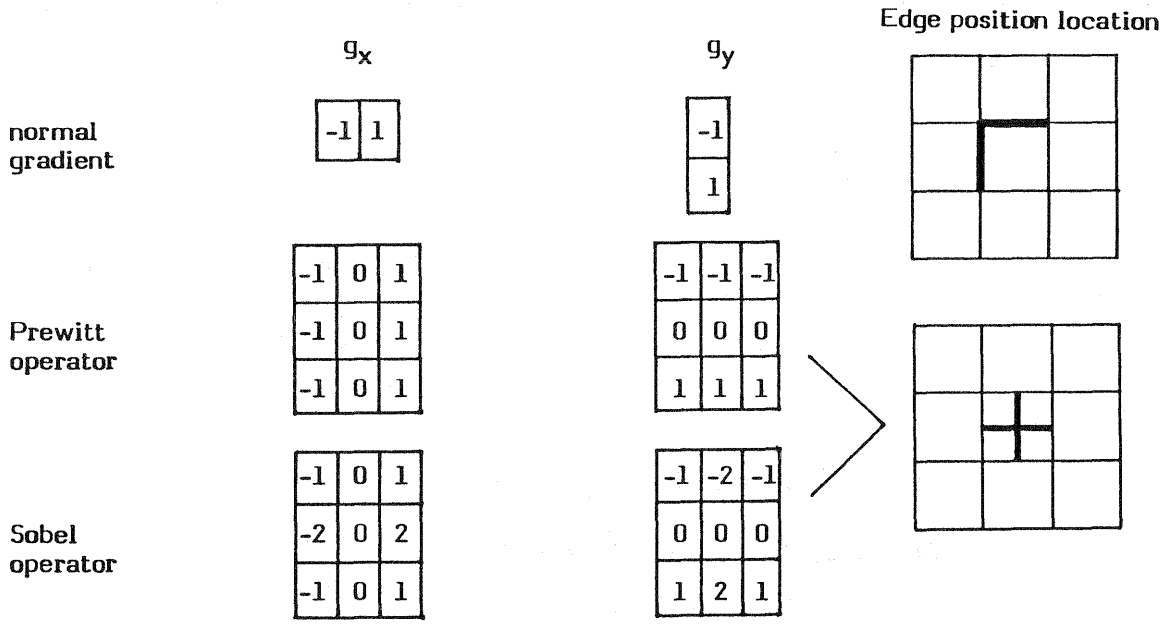

Fig. 3 The masks and edge location of the investigated edges

2.2 Smoothing filters

Since, in general, image data will be corrupted by some kind of anomalies, often prior to segmentation, enhancement techniques are employed to reduce the effect of these anomalies. Smoothing is such a preprocessing techniques, aiming to diminish the noise portion in a signal.

Many preprocessing methods may improve the subjective quality of images, but actually degrade the image for further digital processing (Yang and Huang, 1981). Since smoothing filters are very often applied previous to edge detection, their effect on edge location determination is substantial, when investigating the precision of edge location of edge detectors.

Smoothing filters can be linear or non-linear. The most simple linear filter is just an unweighted averaging over a (e.g. 3 x 3) neighbourhoud. Although linear filters are easy to design, their drawback is that they don't only diminish noise but also edge signal. Furthermore, they only remove noise partially. So, impulse like anomalies are not totally eliminated but just spread out over a larger neighbourhood. In many applications non-linear smoothing can circumvent these problems, since they have edge preserving properties; i.e. impulse noise is removed without corroding edges.

Three non-linear smoothing filters are incorporated into the present investigation for analysis:

- median filter;
- edge preserving filter;
- conditional average filter.

The median filter and the edge preserving filter are objective since they don't need human intervention. The conditional average filter requires a threshold, which introduces a subjective element. The median filter is thoroughly investigated (see, e.g. Yang and Huang, 1981; Bovik et al., 1987). The filter has been observed to be very efficient for especially impulse noise removal without perturbing edges. Our investigation affirms this observation. The above filters aren't treated here in more detail. A detailed treatment is given in Lemmens et al. (1988).

Although it is not uncommon in digital image processing to employ smoothing filters several times in succession before segmentation takes place, we just employ the smoothing filters once.

3 Test Image and Figures of Merit

First the creation of the ideal image is considered, next the artificial degradation of the image is looked at and the section closes with the treatment of some figures of merit, describing precision and reliability.

3.1 Creation of the ideal test image

To carry out experiments, a synthetic image (size 128 x 128 pixels), consisting of triangles is created. The design and performance of the image depends on the following characteristics that may affect edge detection:

- isotropy;
- edge type response;
- dynamic range of grey value differences.

The isotropy condition requires that the polygon configuration can be rotated with respect to the raster underground. As edge type response just ideal step edges are considered at the moment. The grey values of the background and the polygonial objects should be changeable to fulfil the last condition. The creation of the ideal image requires also that the polygons have to intersect with the rasterline of the image matrix in order to compute the "exact" grey value of the mixed pixels. Mixed pixels lie partially in the background and partially in the object. At vertices the kind of intersection has to be defined for each type of intersection individually. The area weights the grey values, i.e. the grey value of a mixed pixel g_m is computed from (remark: each pixel is considered to be of unit area):

$$g_m = A\, g_o + (1 - A)\, g_b$$

with: A: the area part of the pixel belonging to the object;
g_o: grey value of the object;
g_b: grey value of the background.

In the present investigation the grey value of the objects is set to 150 and that of the background to 50.

Several shapes and sizes of triangles are used. The shape is defined by the angles: ϕ_i, i = 1, 2, 3; $\Sigma\phi_i = 180^o$. To achieve an economical set up, the following angles are chosen:

ϕ_1	ϕ_2	ϕ_3
140^o	20^o	20^o
120^o	20^o	40^o
100^o	20^o	60^o
80^o	40^o	60^o

Six sizes are used. The largest linear extent is about 30 pixels, the smallest about 5 pixels. The triangle (140^o, 20^o, 20^o) vanishes in the smallest size. So, the total configuration exists of 23 triangles, shown in fig. 4.

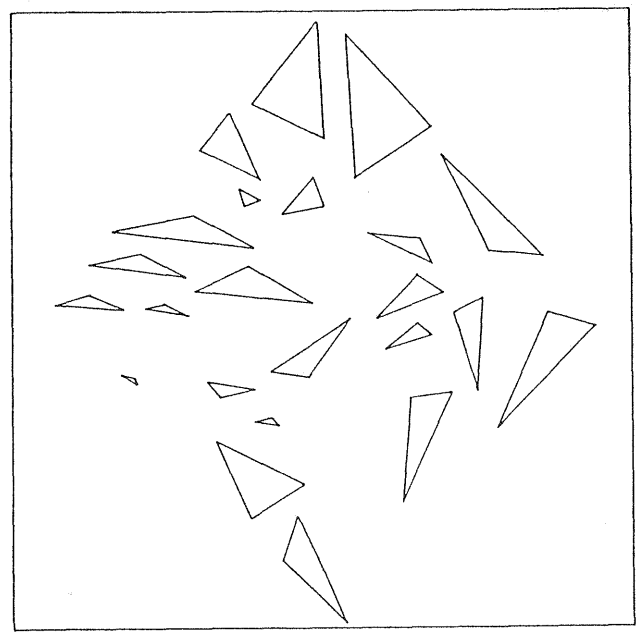

Fig. 4 The configuration of the ideal image

3.2 Degradation

The degradation of the artificial ideal image -blur, Gaussian noise and impulse noise- is simulated by computer. Some sources of blur are, e.g.: atmosphere, finite sensor apperture, optical aberrations and defocussing. It is assumed that the point spread function (PSF) of the imaging system, responsible for blur, can be approximated by a discrete 2-D Gaussian (i.e. statistical normal probability density) function. In digital integer domain a Gaussian PSF can be simulated by a repeated convolution of the image with a 2 x 2 unweighted linear smoothing filter, given by the mask:

$$\frac{1}{4}\begin{bmatrix}1 & 1\\ 1 & 1\end{bmatrix}$$

So, the Gaussian PSF of 3 x 3 window is:

$$\frac{1}{16}\begin{bmatrix}1 & 2 & 1\\ 2 & 4 & 2\\ 1 & 2 & 1\end{bmatrix}$$

Part of the noise is considered as additive zero-mean Gaussian $N(0,\sigma)$, which simulates, among others, the thermal noise in electrical circuits. The other part of the noise is impulse noise, simulating defective sensors. Noise caused by bit reversal during signal transfer is foreseen but not yet implemented. Both Gaussian noise and impulse noise are simulated by application of a random number generator. The effect of the above distortions on an ideal step edge is demonstrated in fig. 5.

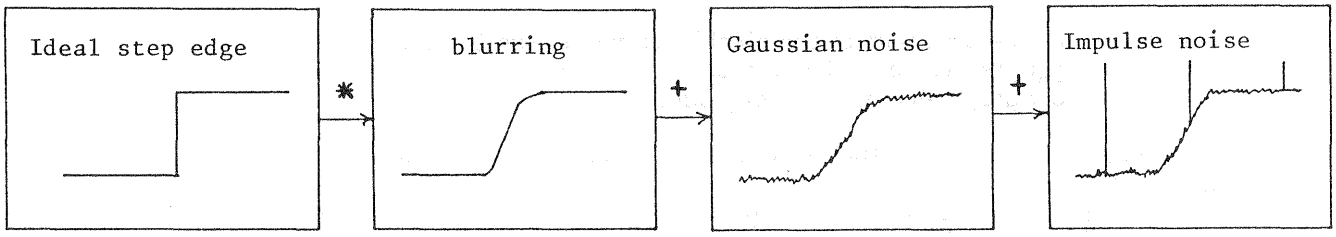

Fig. 5 Illustration of the present simulated degradations on an ideal step edge

3.3 Figures of Merit

There are two principal criteria relevant to edge detection:

- edgels should be well localized, i.e. the detected position between the ideal boundaries and the detected one should be as minimum as possible;
- all relevant edgels should be detected and false edge detection should be avoided.

Both criteria define the accuracy of edge detection. The first criteria refers to precision and the second one to reliability. Most former investigations on the accuracy of edge detection have considered the reliability aspect. This paper emphasizes the precision.

Before figures of merit can be given, first a definition about 'edge position' has to be given. Differential-type of edge detectors determine edgels just at pixel level. To achieve subpixel level, some kind of interpolation is necessary. The Prewitt and Sobel operator position the edgels at the mid point of the image pixel that corresponds to the mid pixel of the g_x and g_y masks. Although the Normal gradient operator positions g_x and g_y at the boundary between the two involved image pixels (see fig. 3) also for this operator the mid point is choosen as representative point.

Reliability measures R_i may look at the following edge detection characteristics:

1 The ratio of the number of detected edges that are part of the ideal boundaries (N_d) to the total number of edges on the ideal boundaries (N_i):

$$R_1 = \frac{N_d}{N_i}$$

2 The ratio of the edge positions which are wrongly detected (N_w) to the total number of edges on the ideal boundaries (N_i):

$$R_2 = \frac{N_w}{N_i}$$

3 The ratio of the number of edges which coincide with the ideal boundaries (N_d) to the number of wrongly detected edges (N_w):

$$R_3 = \frac{N_d}{N_w}$$

4 The ratio of some function of the number of edges which coincide with the ideal boundaries (N_d) and the number of wrongly detected edges (N_w) to the total number of edges on the ideal boundaries (N_i). We propose the following measure:

$$R_4 = \frac{N_d - \alpha N_w}{N_i}$$

with α a weighting factor which depends on the importance of the effect of the number of undetected edges and of the number of wrongly detected edges on further processing.

Defining dL_i as the distance between the position of the detected edge and the ideal boundary, the following precision measures M_i are defined:

1 The mean distance (deviation) between the detected edges, coinciding with the ideal boundaries and the real position of the boundaries:

$$M_1 = \frac{1}{N_d} \sum_{i=1}^{N_d} dL_i$$

2 The variance, i.e. the mean of the squared distances (deviations) between the detected edges and the ideal boundaries:

$$M_2 = \frac{1}{N_d} \sum_{i=1}^{N_d} (dL_i)^2$$

The above figures describe precision and reliability separately. A figure which mixes both into one measure, is Pratt's figure of merit (c.f. Abdou and Pratt, 1979):

$$F = \frac{1}{N_a} \sum_{i=1}^{N_a} \frac{1}{1 + \alpha (dL_i)^2}$$

with: $N_a = \max(N_d, N_i)$ and α a weighting factor to provide a relative penalty between smeared edges and isolated, but offset, edges. It is often set to 1/9 (Abdou and Pratt, 1979). F lies between 0 and 1; 0 is a bad and 1 a good figure. Peli and Malah (1982) have observed that Pratt's figure of merit isn't adequate, since it favours precision at the cost of reliability. This point is discussed in the next section.

In the present investigation M_1 is employed. None of the above reliability measures is applied explicitly, just N_d is listed. However, by comparing N_d with the number of detected edges coinciding with boundaries in the ideal image, a reliability measure is obtained.

4 Experimental results and discussion

The numerical results of the accuracy analysis are presented in table 1 and 2, and are further graphical presented in fig. 6-9. To fig. 8 and 9 belongs the following legend:

Ideal boundaries superimposed on ideal image convolved with edge detector (edge image)	Ideal image convolved with edge operator (edge image)	edge image of ideal image corrupted by: - Gaussian noise (20) - 5% impulse noise
median filter applied on degraded image and and next convolved with edge operator	edge pres. filter applied on degraded image and next convolved with edge operator	cond. aver. filter applied on degraded image and next convolved with edge operator

Ideal image

	no smooth.		median		edge-pres.		cond.	
	m_1	n	m_1	n	m_1	n	m_1	n
P	0.40	1012	0.42	928	0.46	1116	0.40	993
S	0.39	990	0.42	924	0.46	1148	0.39	992
G	0.40	588	0.41	452	0.42	718	0.37	620

Impulse noise 1 %

	no smooth.		median		edge-pres.		cond.	
	m_1	n	m_1	n	m_1	n	m_1	n
P	0.43	1032	0.42	927	0.46	1108	0.40	1005
S	0.43	1019	0.42	922	0.46	1140	0.40	1005
G	0.44	639	0.41	449	0.43	730	0.37	607

Gaussian noise: sigma = 5

	no smooth.		median		edge-pres.		cond.	
	m_1	n	m_1	n	m_1	n	m_1	n
P	0.40	1005	0.40	873	0.46	1118	0.40	996
S	0.39	998	0.39	879	0.46	1159	0.40	1007
G	0.40	597	0.37	420	0.42	727	0.38	651

Impulse noise 5 %

	no smooth.		median		edge-pres.		cond.	
	m_1	n	m_1	n	m_1	n	m_1	n
P	0.50	1140	0.42	943	0.46	1081	0.44	1045
S	0.51	1162	0.42	938	0.46	1111	0.44	1042
G	0.51	816	0.42	462	0.49	799	0.43	685

Gaussian noise: sigma = 10, Impulse noise 5 %

	no smooth.		median		edge-pres.		cond.	
	m_1	n	m_1	n	m_1	n	m_1	n
P	0.54	1214	0.41	825	0.46	1043	0.48	1063
S	0.55	1225	0.41	851	0.46	1094	0.49	1077
G	0.53	862	0.44	394	0.48	766	0.45	719

Gaussian noise: sigma = 10

	no smooth.		median		edge-pres.		cond.	
	m_1	n	m_1	n	m_1	n	m_1	n
P	0.41	1031	0.39	624	0.46	1086	0.41	1006
S	0.41	1022	0.39	825	0.46	1134	0.41	1016
G	0.40	624	0.39	374	0.41	715	0.40	674

Gaussian noise: sigma = 10, Impulse noise 5 %, Blur 3x3

	no smooth.		median		edge-pres.		cond.	
	m_1	n	m_1	n	m_1	n	m_1	n
P	0.58	785	0.30	315	0.40	722	0.46	539
S	0.60	850	0.31	347	0.41	759	0.45	577
G	0.77	262	0.60	10	0.49	568	0.51	197

Gaussian noise: sigma = 20

	no smooth.		median		edge-pres.		cond.	
	m_1	n	m_1	n	m_1	n	m_1	n
P	0.45	1015	0.39	633	0.46	1026	0.45	974
S	0.44	1017	0.40	656	0.46	1055	0.42	956
G	0.52	792	0.38	216	0.44	689	0.48	674

Table 1

Gaussian noise: sigma = 10; Impulse noise 2 %

	no smooth.		3x3 Gauss.		median		edge-pres.		cond.	
	m_1	n	m_1	n	m_1	n	m_1	n	m_1	n
P	0.43	1068	0.41	998	0.40	834	0.46	1067	0.40	1004
S	0.43	1064	0.40	994	0.40	855	0.46	1110	0.41	1014
G	0.43	661	0.40	593	0.39	377	0.41	711	0.40	672

Table 2

Legend to table 1 and 2

P: Prewitt operator
S: Sobel operator
G: Normal gradient operator

m_1: precision measure 1: mean distance of detected edges to ideal boundaries
n: number of detected edges which coincide with ideal boundaries (real edges); compare with N_d in text.

The other abbrevations are self-contained.

Table 1 shows that also for the ideal (i.e. non-degraded) image, the application of non-linear smoothing filters affect the number of detected edges on ideal boundaries (N_d) with respect to the non-smoothing case. The median filter decreases N_d considerably. The table shows that this is a general property of the median filter.

Fig. 6 shows that the precision decreases for any type of differential edge detector with increasing impulse and Gaussian noise. Fig. 7 shows the behaviour of the non-linear smoothing filters under several impulse and Gaussion noise conditions. The median and edge preserving filter are consistent. The conditional average filter has median-like characteristics under low noise conditions and evolves to edge preserving characteristics with increasing noise.

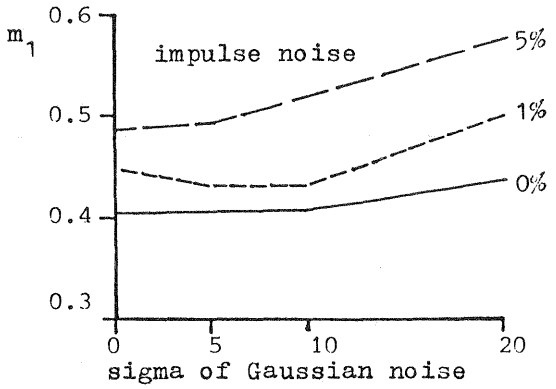

Fig. 6 The precision according to measure 1 (M_1) decreases for any type of differential edge detector with increasing impulse and Gaussian noise.

The median filter shows the best precision properties. However, table 1 and fig. 8 and 9 show that many edges stay undetected, i.e. the median filter isn't reliable with respect to N_d. At the other side the number of wrongly detected edges is very low, i.e. the median filter is reliable with respect to N_w.

The edge preserving filter augments often the number of detected edges, compared with the non-smoothing case, even for the ideal image. The filter preserves much more edges from corroding than the median filter, but also more edges are detected wrongly, as can be qualitatively verified in fig. 8 and 9. Furthermore, the edge preserving filter shows bad precision characteristics, although consistent. Even under very heavy noise conditions it isn't remarkable less than in sligthly degraded images. Also N_d is largely indepent of noise conditions. Under slight noise the conditional average filter shows the best properties, for both precision and N_d properties. The filter has the drawback that it needs the adjustment of a threshold, which requires experiments.

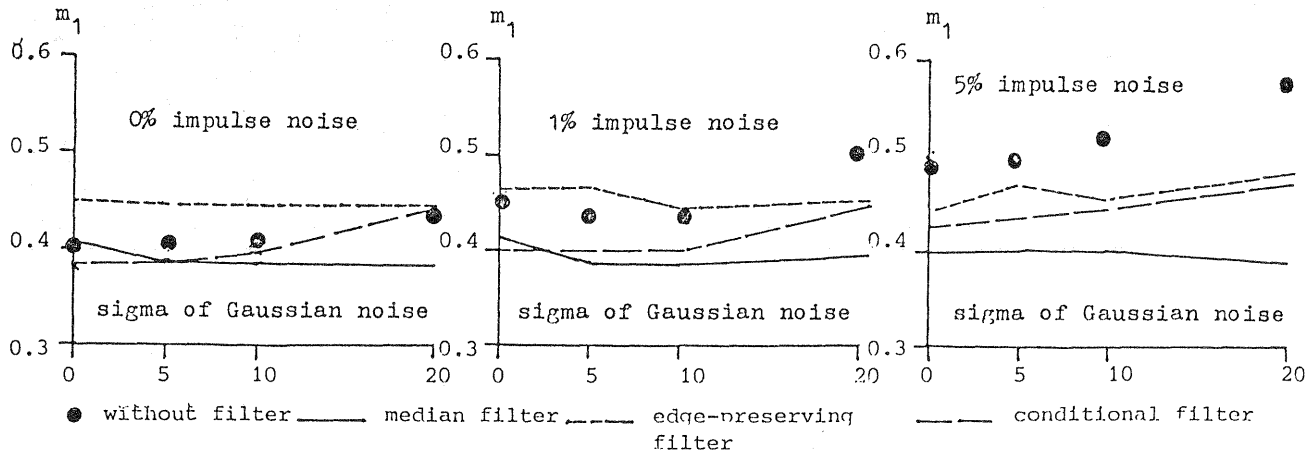

Fig. 7 Effect of non-linear smoothing on edge location precision with increasing Gaussian and impulse noise

Under nearly noise free conditions, the Normal gradient operator shows the best results. The operator is small, determines just single edges and is computationally efficient. It is remarkable that even in case of 5% impulse noise the combination of Normal gradient and conditional averaging filter show a high precision, while the number of undetected edges is low. The disadvantage of this combination is however that many edges are wrongly detected as can be qualitatively indicated in fig. 9. So, the method is an appropriate one when boundary detection is carried out by search near an approximate boundary location.

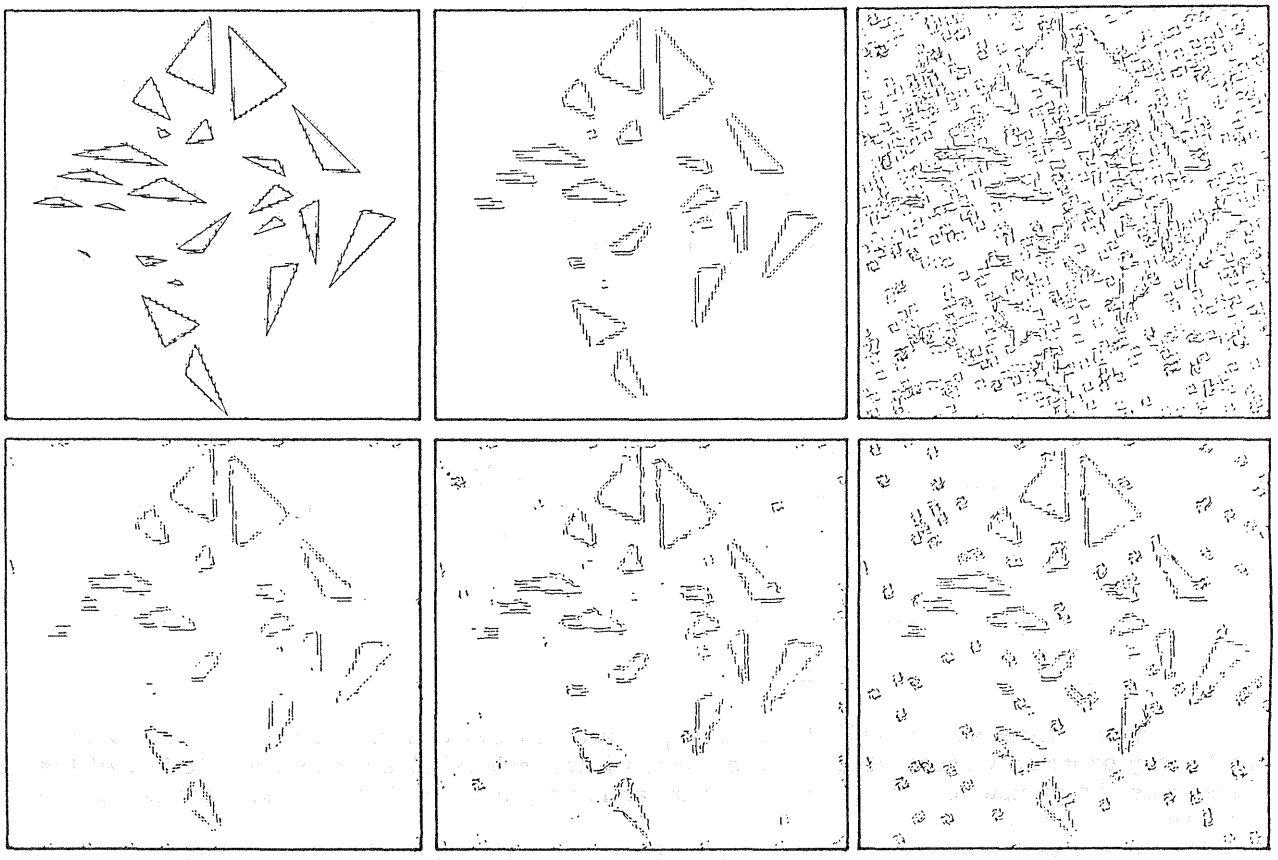

Fig. 8 Prewitt operator

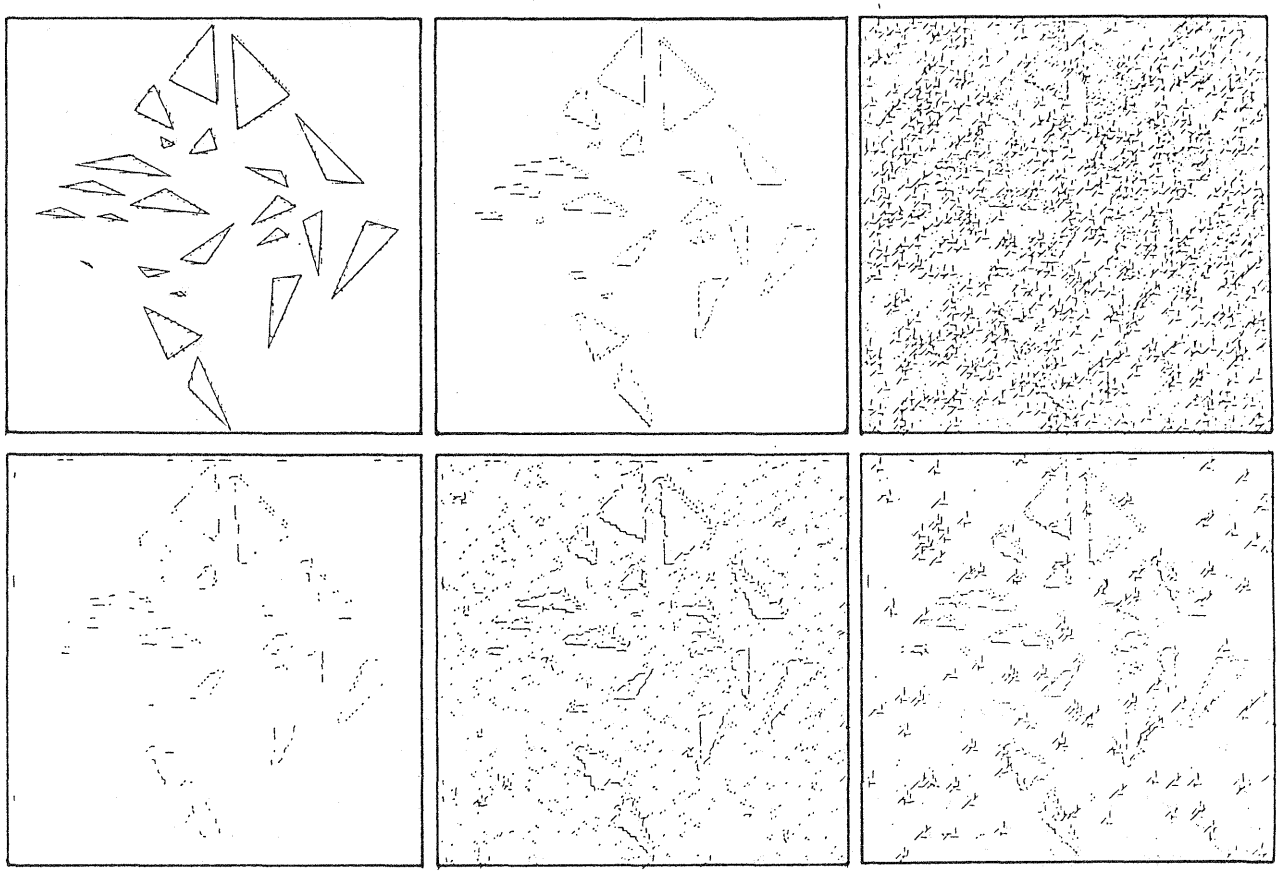

Fig. 9 Normal gradient operator

Even under heavy noise conditions the combination of Normal gradient and edge preserving filter performs well. The Prewitt and Sobel operator show nearly the same characteristics, which is not astonishing when regarding the masks. In general, the choise of the smoothing filter affects much more the accuracy than the kind of edge detector.

For Gaussian noise of sigma = 10 and 2% impulse noise, the effect of non-linear smoothing filters is compared with those of the 3x3 Gaussian smoothing filter (a linear filter). Even with rather strong noise linear smoothing reveals almost the same precision characteristics as the median filter: the precision is slightly improved. This observation corresponds globally with the one of Yang and Huang (1981), who have compared the effect of linear filtering on edge location of one-dimensional signals corrupted by impulse and Gaussian noise. They found that, in general, median filtering preserves step edges better than averaging, but that in the case of Gaussian noise, neither averaging nor median filtering improves the accuracy of step edges.

The threshold on the edge magnitude is experimentally determined from the ideal image, separately for the three detectors. Since blurring causes smearing of the edges over several pixels and consequently decreases the edge strength, no thoroughly insight on the effect of blurring is obtained at present.

Peli and Malah (1982) have observed that Pratt's figure of merit may give a high response even when the number of undetected edges is high. Furthermore, the squared distance dL_i^2 in the denominator, causes that small edges are preferred. So, the measure favours precision with respect to reliability. Our conclusion is that edge location accuracy can not be expressed by just one measure; it needs two measures, one for precision and one for reliability. As precision measure, the variance (M_2 in the previous section) has to be further investigated. In the previous section also a suggestion is given for a new reliability measure, which incorporates both the rightly and wrongly detected edges.

5 Conclusions

The edge location accuracy of the Prewitt, Sobel and Normal gradient operator in combination with non-linear smoothing filters are quantitatively and qualitatively compared under several noise conditions. Also comparisons with a 3x3 Gaussian filter are carried out. From the simulations executed on synthetic images, the following may be concluded.

The median filter gives under heavy noise conditions the best results with respect to precision and wrongly detected edges. But many edges remain undetected. It should be used when wrong edge detection causes much more severe problems than a large number of undetected edges. For nearly noise free images with ideal step edges the normal gradient shows the best results. The Normal gradient has, like the Roberts' operator, a small size. Peli and Malah (1982) conclude from their simulations that the Roberts' operator is the best one to use for an image with a small amount of noise and rather steep ramp edges. Under heavy noise conditions the Normal gradient performs well, if the image is first preprocessed with the edge preserving or conditional average filter. So, small detectors are, in general, preferable to larger ones, but noise reduction by smoothing is necessary.

Former investigations tried to express the accuracy in one type of measure, i.e. the precision is not separated from reliability. A separation between both is necessary. A new reliability measure is suggested.

References

Abdou, I.E., Pratt, W.K., 1979, Quantitative design and evaluation of enhancement/thresholding edge detectors, Proc. of the IEEE, vol. 67, no. 5, pp. 753-763.

Bovik, A.C., Huang, T.S., Munson, D.C., 1987, The effect of Median filtering on edge estimation and detection, IEEE Trans. Pattern analysis and machine intelligence, vol. PAMI-9, no. 2, pp. 181-194.

Davis, L.S., 1975, A survey of edge detection techniques, Computer graphics and image processing, vol. 4, pp. 248-270.

Davis, E.R., 1986, Constraints on the design of template masks for edge detection, Pattern recognition letter, pp. 111-120.

Förstner, W., 1986, a Feature based correspondence algorithm for image matching, Int. Arch. of Photogr. vol. 26-III, Rovaniemi, pp. 1-17.

Haralick, R.M., 1980, Edge and region analysis for digital image data, Computer graphics and image processing, vol. 12, pp. 60-73.

Haralick, R.M., 1983, Ridges and valleys on digital images, Computer vision, graphics, and image processing, vol. 22, pp. 28-38.

Hueckel, M.H., 1973, A local visual operator which recognizes edges and lines, Journ. ass. computing machinery, vol. 20, no. 4, pp.634-647.

Lemmens, M.J.P.M., 1988, GIS-digital image interaction, Archives of the 16th ISPRS Congress, comm. IV, Kyoto, Japan.

Lemmens, M.J.P.M., Bruel, E.W., Fennis, F., 1988, Linear feature extraction and road recognition from large scale digital aerial images, Archives of the 16th ISPRS Congress, comm. VII, Kyoto, Japan.

Marr, D., Hildreth, E., 1980, Theory of edge detection, Proc. R. Soc. Lond. vol. B 207, pp. 187-219.

Morgenthaler, D.G., 1981, A new hybrid edge detector, Computer graphics and image processing, vol. 16, pp. 166-176.

Peli, T., Malah, D., 1982, A study of edge detection algorithms, Computer graphics and image processing, vol. 20, pp. 1-21.

Rosenfeld, A., Kak, A.C., 1982, Digital picture processing, Academic Press, New York.

Sethi, I.K., 1982, Edge detection using charge analogy, Computer graphics and image processing, vol. 20, pp. 185-195.

Shaw, G.B., 1979, Local and regional edge detectors, some comparisons, Computer graphics and image processing, vol. 9, pp. 135-149.

Smith, M.W., Davis, W.A., 1975, A new algorithm for edge detection, Computer graphics and image processing, vol. 4, pp. 55-62.

Tabatabai, A.J., Mitchell, O.R., 1984, Edge location to subpixel values in digital imagery, IEEE Trans. Pattern analysis and machine intelligenc, vol. PAMI-6, no. 2, pp. 188-201.

Torre, V., Poggio, T.A., 1986, On edge detection, IEEE Trans. Pattern analysis and machine intelligence, vol. PAMI-8, no. 2, pp. 147-163.

Yang, G.J., Huang, T.S., 1981, The effect of median filtering on edge location estimation, Computer graphics and image processing, vol. 15, pp. 224-245.